High-tech composites to ancient metals

Neutron diffraction methods offer a direct measure of the elastic component of strain deep within crystalline materials through precise characterisation of the interplanar crystal lattice spacing. The unique non-destructive nature of this measurement technique is particularly beneficial in the context of engineering design and archaeological materials science, since it allows the evaluation of a variety of structural and deformational parameters inside real components without material removal, or at worst with minimal interference. We review a wide range of recent experimental studies using the Engin-X materials engineering instrument at the ISIS neutron source and show how the technique provides the basis for developing improved insight into materials of great importance to applications and industry.

S.Y. Zhang[1], E. Godfrey[1], W. Kockelmann[1], A. Paradowska[1], M. J. Bull[1], A. M. Korsunsky[2], B. Abbey[2], P. Xu[3,4], Y. Tomota[3], D. Liljedahl[5], O. Zanellato[5], M. Fitzpatrick[5], M. R. Daymond[6], R. M. Toda[6], R. A. Holt[6], J.Kelleher[7], S. Siano[8], J. Santisteban[9]

[1]*ISIS Pulsed Neutron and Muon Source, Science and Technology Facilities Council, Rutherford Appleton Laboratory, Didcot, Oxfordshire, UK*

[2]*Department of Engineering, University of Oxford, Oxford, UK*

[3]*Graduate School of Science and Engineering, Ibaraki University, 4-12-1 Nakanarusawa, Hitachi, 316-8511, Japan;*

[4]*Quantum Beam Science Directorate, Japan Atomic Energy Agency, 2-4 Shirane Shirakata, Tokai-mura, Naka-gun, Ibaraki, 319-1195, Japan*

[5]*The Faculty of Mathematics, Computing and Technology, Open University, Milton Keynes, UK*

[6]*Department of Mechanical and Materials Engineering, Queen's University, Kingston, Canada*

[7]*School of Materials, University of Manchester, Manchester, UK*

[8]*Istituto di Fisica Applicata 'Nello Carrara'—CNR, Via Madonna del Piano, 50019 Sesto Fiorentino, Italy*

[9]*Laboratorio de Fisica de Neutrones, Centro Atomico Bariloche (R8402AGP), San Carlos de Bariloche, Argentina*

A variety of strain measurement techniques have evolved over the decades and are widely employed in experimental studies of deformation behaviour of materials and structures. The aim of strain measurement is to characterise the response to applied loads, particularly those corresponding to in-service loading, and to observe the response of objects so as to predict the integrity of various designs. This is the principal significance of strain analysis for structural design[1].

Most strain measurement methods are only capable of measuring total strain increments. This is due to the fact that strain measurement

ISSN:1369 7021 © Elsevier Ltd 2009

is usually accomplished by monitoring the change of distance between reference points associated with markers placed on the surface or embedded in the bulk of the material. This distance is affected by both the elastic and inelastic parts of strain. Examples of experimental techniques include contact methods, such as clip gauges or resistive strain gauges[2], and non-contact methods, such as photogrammetry (measurement of displacements of visible grids on sample surface), Moiré interferometry methods that make use of reflective gratings deposited on sample surface[3], and Digital Image Correlation (DIC) methods[4].

The particular significance of neutron and X-ray diffraction methods is that they offer a direct method of measuring the *elastic* component of strain deep within crystalline materials through the precise characterisation of the interplanar crystal lattice spacing. In contrast with the other methods mentioned above, diffraction uses the atomic lattice itself as a deformation gauge. This makes the methods sensitive only to elastic strains, since inelastic strain mechanisms do not induce changes in interplanar lattice spacing: plasticity causes lattice plane shear, while damage causes voiding i.e. lattice plane separation (to distances that far exceed the original spacing).

Since stress is directly related to elastic strain, with the knowledge of the material stiffness, diffraction thus provides a highly precise, spatially and directionally resolved means of stress evaluation. Thanks to its stress evaluation capability, diffraction has become an increasingly important tool in engineering. Since most criteria of integrity and failure in structural engineering use stress as the key parameter, diffraction methods have become useful in predicting the durability of components, optimising design and improving performance. The unique non-destructive nature of this measurement technique is particularly beneficial in the context of engineering design, since it allows the evaluation of a variety of structural and deformational parameters inside real components without material removal, or at worst with minimal interference. Further, the combination of rapid data collection with good penetration depths allows in situ, real time, spatially resolved strain measurement (mapping) under the conditions representative of those that might be experienced in service to investigate the microstructure evolution behaviours involving phase transformations[5,6], bulk texture evolution[7], heterogeneous elastic/plastic deformation[8,22], and dynamic recrystallization[9,10].

The principle of diffraction strain measurement in polycrystalline alloys relies on Bragg's law that establishes the relationship between the average interplanar lattice spacing d within the measurement gauge volume:

$$2d \sin \theta = \lambda \tag{1}$$

When a polycrystalline aggregate deforms elastically, the interplanar spacing within the constituent grains changes. Within a set of planes that have similar orientation with respect to the stress direction, the interplanar spacing is similar between one grain and another. This grain-set-specific strain causes observable shifts of powder-like diffraction peaks, i.e. peaks obtained from the superposition of reflections from multiple grains. The average values of lattice spacing extracted from diffraction peak analysis are then compared to the spacing of the same planes measured in an unstressed sample d_0. Average elastic strain can be found from deformed lattice spacing d by

$$\varepsilon = \frac{(d - d_0)}{d_0} = \frac{\Delta d}{d_0} \tag{2}$$

Engin-X at ISIS

The Engin-X instrument at ISIS is a world leading neutron diffractometer purpose-built for stress evaluation in the context of materials engineering and research. Engin-X is very popular and used extensively by both engineers and materials scientists. Measurements are carried out in collaborative experiments between universities, industry and ISIS to address a wide range of engineering problems: new welding technologies for airframe manufacturing; fatigue crack initiation and propagation in composite materials; thermal cycling of materials used in the power generation industry; and the development of strain measurement standards.

Because the method is non-destructive and Engin-X is able to accommodate large intact objects, archaeological materials scientists, conservators, and technical art historians also find that the instrument provides them with data on metal artefacts that they could not acquire by conventional means. The alternative, traditional methods of microstructure determination require invasive sampling. Because of this, strain and tensile tests for example have in the past very rarely been done on archaeological and historic objects.

A sample mounting stage allows samples weighing up to one tonne to be accurately positioned within the measurement point with the accuracy better than 10 µm. Moving and rotating the sample within the neutron beam allows spatial and directional maps of strain to be built up. With the large sample mounting space, Engin-X provides the flexibility for the users to bring their own ancillary devices, such as welding rigs to perform real-time strain measurements during joining. An in situ mountable servo-hydraulic stress rig can apply up to 100 kN tensile or compressive cyclic loads. The rig is equipped with a furnace and a cryogenic chamber that allow the sample to be maintained at temperatures from -200 °C to 1100 °C within normal atmosphere or under inert gas. The automation of experimental setup for complex shape samples can be addressed via the use of the coordinate measurement machine (CMM), laser scanning inspection arms, a robotic arm and the virtual laboratory, SScanSS[11].

With regard to Heritage Science applications, diffraction measurements without any sample environment can be carried out on the actual artefact itself, although it is important to have comparative replica measurements too, as all early metal objects are effectively 'unknown' samples, each made individually in the days before industrial standardisation. The chemical composition of the metal object has to be characterised first, then replicas produced of the same composition and dimensions (in particular, thickness). The replicas must be formed in the way(s) that the original was likely to be produced, e.g. casting, hammering, fire-welding. The replicas can then be tested under different environments. The results are compared with the data obtained from the archaeological artefact, and interpretations can be made about how the original object was produced. Archaeometallurgy is very often in effect 'reverse engineering'.

A comprehensive introduction to the neutron strain scanning technique can be found in Hutchings *et al.*[12]. A description of the state-of-the-art in stress measurement using neutron and synchrotron radiation is contained in Fitzpatrick and Lodini[13]. More information about Engin-X can be found in Santisteban *et al.*[14].

Ferrite transformation in low alloy steels

The deformation-induced ferrite transformation is well known as one of the most economical ways to refine the microstructures of modern high strength low alloy steels. The effects of deformation temperature, strain and strain rate on dynamic ferrite transformation during hot deformation have been investigated in the last decade indirectly, whereby the microstructure is examined after interrupting hot deformation at different strains, and quenching deformed specimens[15,16].

The temperature control and the hot deformation processing history of a low alloy steel (2% Mn and 0.2% C by weight) in the as-quenched condition are shown in Fig.1. The effect of compressive deformation on the isothermal ferrite transformation at different temperatures is shown in Fig. 2. If no hot deformation is applied, the ferrite volume fraction increases gradually with increasing isothermal hold time, and the static ferrite transformation is accelerated evidently by lowering

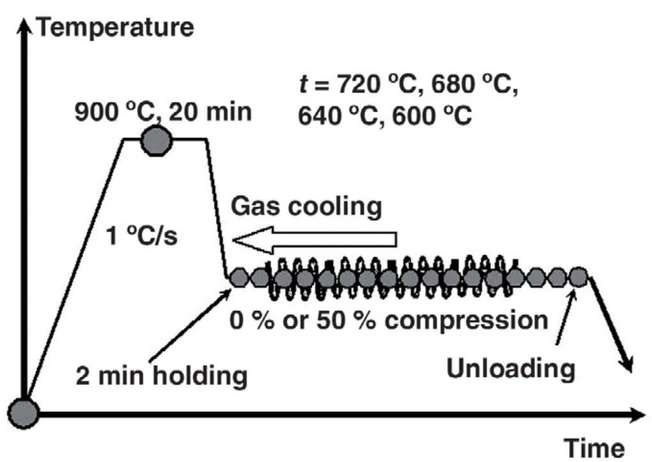

Fig. 1 Schematic illustration for the temperature control and hot deformation process.

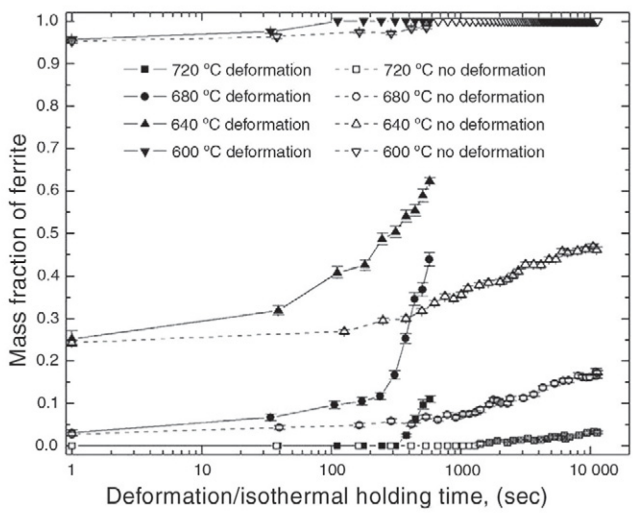

Fig. 2 Change in ferrite amount during ferrite transformation.

the holding temperature. In the case of hot deformation, it is found that it promotes the ferrite transformation in the dual phase region (600 °C, 640 °C, and 680 °C) as well as in the single phase austenite region (720 °C), i.e. the occurrence of dynamic ferrite transformation has been confirmed at different transformation temperatures. Such changes in the dynamic ferrite transformation kinetics are believed to be related to the carbon concentration and the volume fraction of austenite, the transformation driving force, and the heterogeneity of plastic deformation.

Residual stresses at cruising altitude temperature

Due to the recent marked progress in cryogenic technologies, there has been a growing interest in material mechanical behaviour at cryogenic temperatures. Applications include cryogenic processing of zirconium nuclear alloys, strain sensitivity of superconducting magnet wires, cryogenic structural steels and low temperature shape memory alloys for space applications.

Until recently, there has been a little capability for in situ diffraction studies of mechanical behaviour at temperatures below ambient[18]. A novel cryogenic experimental device has been developed consisting of a vacuum chamber with cooling provided by a closed cycle refrigerator down to –200 °C in samples under applied loads of up to 100 kN[19].

In order to reduce weight, modern aircraft components are increasingly becoming hybrid structures of fibre reinforced plastics and metallic parts[20]. Such structures present a lot of advantages over traditional ones. However the difference of coefficient of thermal expansion between the materials causes tensile residual stresses in the metallic parts. This might affect the fatigue resistance. The stresses introduced by the thermal mismatch will change with the temperature. At the cruising altitude of 10 000 m, the atmosphere temperature is around -50 °C, and the tensile residual stresses are much higher than at ground level temperature.

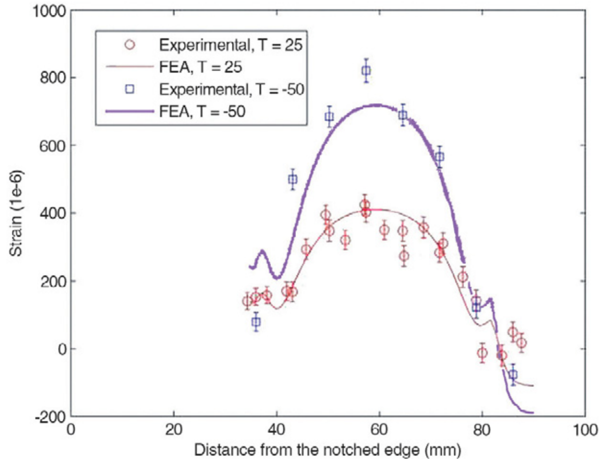

Fig. 3 Residual stress in a compact tension specimen 3.5 mm below the bonded interface, at room temperature and flight temperature, compared with FEA modelling.

Liljedahl *et al.*[21] studied an aluminium alloy compact tension specimen adhesively reinforced with a 2 mm titanium strap. The adhesive was cured at 120 °C and strain measurements were carried out at room temperature and -50 °C. Residual stresses were found to be about 40 MPa at room temperature and about 70 MPa at -50 °C. Residual strains in the specimen were modelled with an elastic finite element representation of the specimen (Fig. 3) and the linear model accurately represents the residual stresses at both temperatures.

Effect of welding procedures on residual stress

Welding is an important industrial joining process, and over the years many different "flavours" of this method have been proposed. For steel components, a bead of molten filler metal is deposited in one or more passes between two edges to be joined, and allowed to solidify. During this process, the joint undergoes a complex thermomechanical cycle during cooling. Of particular concern is the formation of tensile residual stress in the weld, which results mainly from thermal contraction as the filler metal cools and hardens. Where several passes are made, a pass may partially relieve the stress in previous passes, creating a complex stress state.

Fig. 4 shows longitudinal strain in two grade 304 stainless steel welds studied by Turski *et al.*[23]. One weld comprises five passes of weld bead to partially fill a groove in a plate, the other weld having eight such passes to completely fill the groove. Additionally, the welding process was stopped and restarted twice during the fifth pass in each sample. First was a 'ramped' stop-start, where the welding power was reduced to zero over a 10 mm length, which was covered again when the welding continued. Secondly, an 'abrupt' stop-start was made by immediately stopping and later restarting the weld.

Although the 8-pass weld was thicker, it was expected that the elastic strains would be lower than in the 5-pass weld, as the final passes would anneal the effect of previous passes. Away from the abrupt stop-start, this is found to be the case. The 8-pass weld has relieved the strain at the ramped stop-start but intensified the strain at the abrupt stop-start. This is attributed to the additional thermomechanical cycling at this point making the material harder and more resistant to the annealing from subsequent passes that occurs elsewhere. The results highlight the need to rigorously specify welding procedures. With experimental results for a given weld, these could predict the effect of changing welding parameters such as the number of passes or the start and stop rates.

In aeroengine manufacturing welding is used widely for the fabrication of shell-like structures such as casings and liners, and in the assembly of compressor and turbine components. Alongside conventional TIG welding, laser welding and friction welding are increasingly used, due to the ability of these methods to join dissimilar materials and to avoid material melting, thus reducing the probability

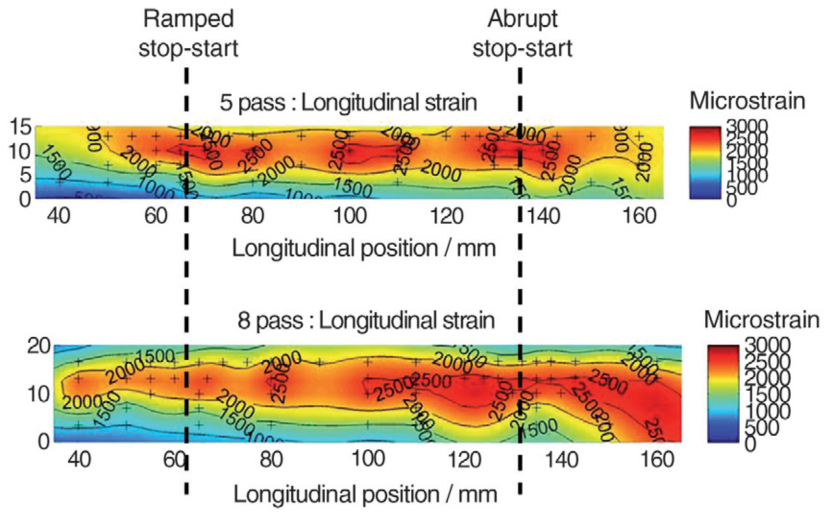

Fig. 4 Strain in the longitudinal direction of a conventional austenitic steel weld made with 5 passes and a similar weld made with 8 passes.

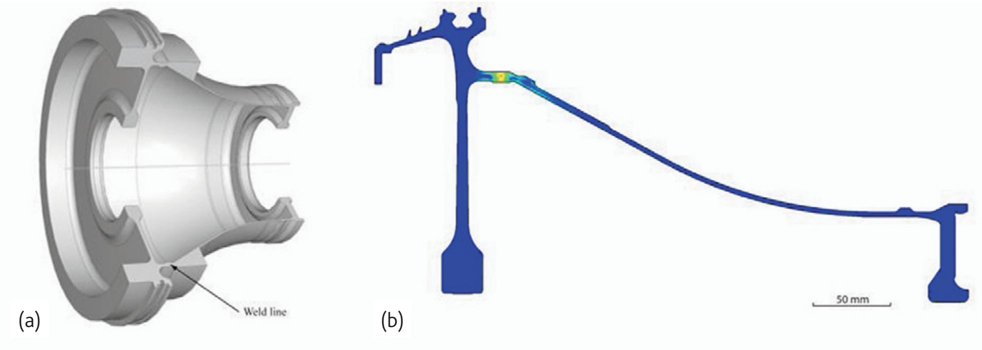

Fig. 5 (a) Schematic diagram of the inertia friction welded high pressure compressor drum – drive cone (DDC) assembly. The circumferential weld line is indicated by the arrow. (b) Illustration of the residual stress map in the DDC in the final post-weld heat treated condition.

of creating defects that may promote crack initiation and propagation. When post-weld heat treatment is applied, there is also the possibility of reducing the "frozen-in" residual stresses usually associated with the bond region and the thermo-mechanically affected zone (TMAZ). Quantification of the residual stresses is an important requirement for improving the design and reliability of the components being joined.

A recent study provides an example of a validated experimental stress analysis basis for structural design of aeroengine assemblies. Strain maps in the vicinity of the bond line of an aeroengine assembly fabricated by inertia friction welding (Fig.5a) can be interpreted using inverse eigenstrain methodology to obtain an approximate reconstruction of the complete residual stress state within the sample[24]. The knowledge of the underlying eigenstrain distributions then allowed the solution to be scaled up to obtain a representation of the residual stress state in the full scale assembly.

Furthermore, subsequent stress relaxation due to creep during post-weld heat treatment can be readily modelled using finite elements. Fig.5b illustrates the computed residual stress state in the full scale assembly following post-weld machining and heat treatment. The predictions have been validated by comparison against various means of residual stress evaluation, including diffraction and hole drilling.

Strain tomography using transmission Bragg edge measurements

A new approach to strain tomography based on energy selective neutron imaging[25] has recently been developed to analyze the residual strain fields by the de-convolution of unknown distributions of residual elastic strains (Fig. 6a). From a data set collected over a range of positions and rotations, the entire strain distribution within the interior of an object can be reconstructed. Using a model-based approach, the unknown strain distribution is represented by a parametric model and solved by minimisation of the mismatch between the simulated and measured data[26,27].

Vorster *et al.*[28] quenched a cylindrical steel sample in water to create a residual stress profile that showed significant hoop compression near the surface, balanced by moderate tension in the core of the sample. Residual hoop and radial strains were measured and the residual stress state simulated by finite element modelling using carefully characterized heat transfer conditions at the sample surface. The residual strains are indicated by the markers in Fig.6b.

The sample was then investigated by neutron transmission Bragg edge measurements using the setup illustrated in Fig.6a. Bragg transmission data were analysed by strain tomography using model-based adaptive mesh approach[27]. The hoop and radial strain distributions were represented by a linear superposition of piecewise linear basis functions, and best match was sought between the predictions and transmission strain measurements. The residual strain profiles reconstructed in this way (Fig.6b) show very good agreement with the known strain fields within the sample measured previously.

Practically, the ability to reconstruct internal strain states from transmission data is likely to open new and exciting possibilities for residual stress analysis, since previously inaccessible configurations may be analysed. Algorithmically, the tomographic reconstruction principle so far has overwhelmingly been used for scalar properties, such as density. Strain, on the other hand, is a multi-component tensor quantity. This presents interesting challenges for the development of this technique. It is important to ensure that the inverse problem addressed is well-posed, either through regularization of the formulation, or by combining transmission data with additional information obtained by other means.

Archaeometallurgy: Manufacturing techniques in Etruscan bronze artefacts

Siano *et al.*[29] studied five archaeological copper alloy objects dated from the 8th to the 4th centuries BC (Fig. 7) from the Marches National Museum of Archaeology, Ancona, Italy, using neutron texture and phase analysis on the Rotax instrument at ISIS, and microstrain measurement on Engin-X. Microstrain measurements were performed at points on the *situla* handle and on the torc, using diffraction and transmission set-ups. The radial scans on the *situla* handle indicated that the preferred orientation was the same, compatible with a cube texture associated with the typical columnar structure that occurs perpendicularly to the

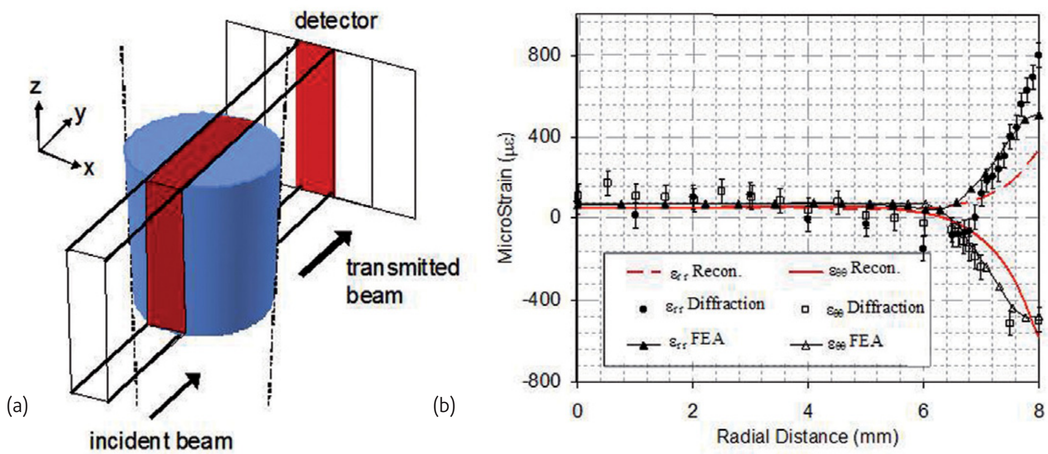

Fig. 6 (a) Illustration of the experimental setup for transmission Bragg edge measurement. (b) The variation of hoop and radial strain components as a function of the radial distance. Strain measured by diffraction are shown by markers (filled circles and hollow squares); finite element modelling results are indicated by triangles. Reconstructed radial and hoop strain distributions are shown by the dashed and continuous lines.

surface of the mould into which the metal is cast. Such a feature was not present in the brazing zone of the handle, which showed random crystal orientation.

A strain map of a selected region around the middle of the torc was calculated by analysis of the Bragg edge shifts (Fig. 8). An inhomogeneous microstrain distribution was found, clear evidence of residual stresses originating from cold deformation of the torc during the final working manufacturing step. Two microstrain profiles along orthogonal directions were also measured where the contribution of eventual plastic deformations due to use was probably negligible. Opposite double-phase modulations were observed along the axial and hoop directions typical of cold bending.

Scans of the *situl*a handle demonstrated that the object was as-cast and did not undergo thermal homogenisation or mechanical treatment. The development of columnar structure in the texture was favoured by the high tin content, corresponding to a relatively low solidification temperature. Conversely, the complex geometry of the brazing and its fast cooling (induced by the metal contact) resulted in a disordered

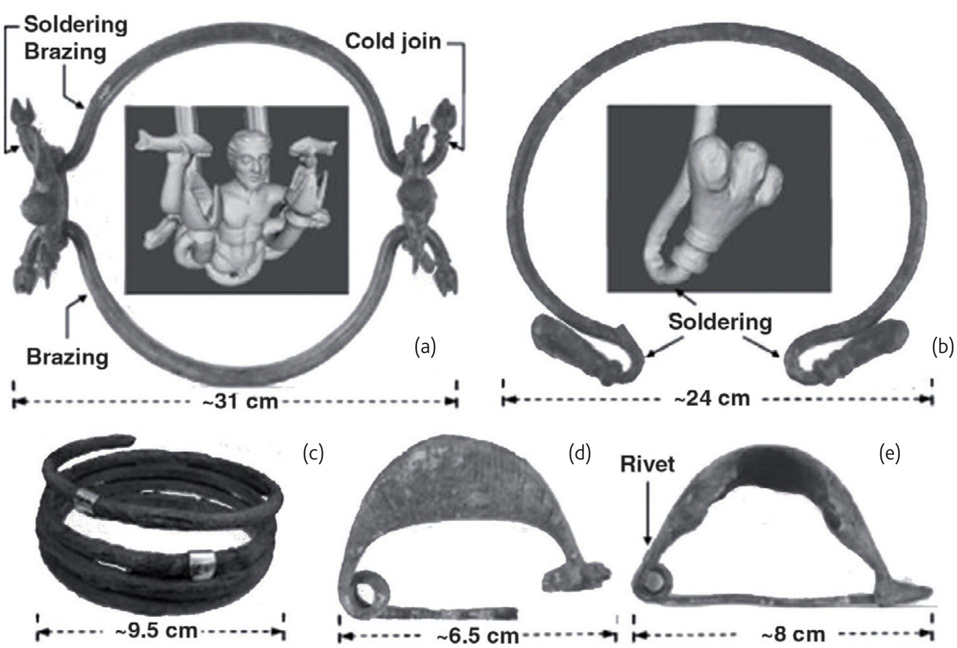

Fig. 7 Etruscan bronze artefacts, from the Marches National Museum of Archaeology, Ancona. (a) a double handle from a situla (bucket); (b) a torc (an object-type that can be interpreted as a neck ornament or a trade-ingot); (c) & (d) bow-fibulae (dress fasteners) and; (e) a bracelet.

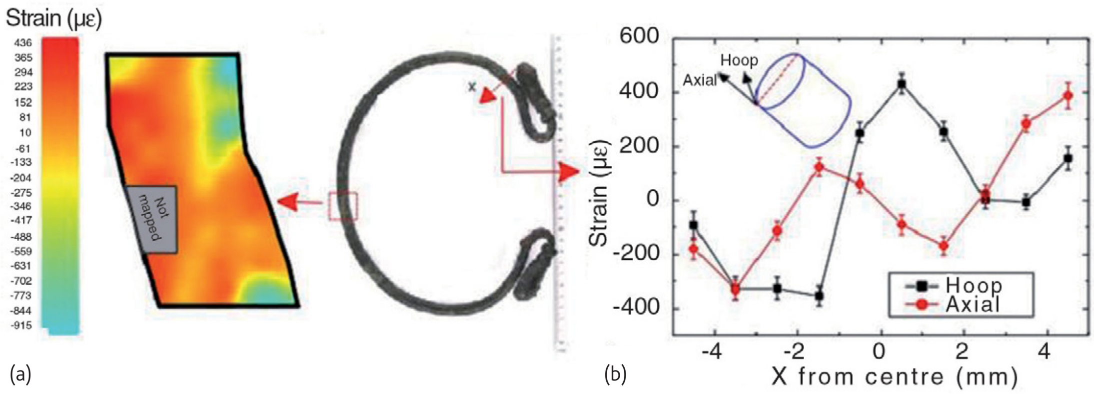

Fig. 8 Residual stresses in the torc: (a) a map of the average microstrains through the bar determined by analysing the Bragg edge shifts (transmission set-up); (b) two orthogonal microstrain profiles in a lateral zone of the bar determined by analysing the shifts of the diffraction peaks.

microstructure. The strain map and scans on the torc demonstrated that it was produced through multiple thermal and mechanical treatments, including a final bending. This suggests that the manufacturing of the object began with the casting of a straight rod, which was then cut and modelled to fit a given diameter (e.g. neck diameter). The final material is elastic rather than plastic, in contrast to the results for the bracelet.

Thus to produce outwardly similar curved shapes of the *situla* handle, the torc, and the bracelet, ancient metalworkers were found to have employed three different sets of procedures.

The future

In order to enhance the neutron imaging capabilities at ISIS and to complement the existing materials analysis facilities, the first neutron tomography instrument at a pulsed neutron source is being designed for the ISIS Second Target Station. The new instrument for materials science & engineering imaging, Imat, will be a state-of-the art combined instrument for cold neutron radiography and diffraction analysis for materials science, materials processing, and engineering studies. The instrument will provide the largest possible neutron flux available for imaging at ISIS and will allow medium-resolution neutron "colour" imaging and diffraction. The ability to perform imaging and diffraction studies on the same beamline with a single sample set-up will offer unprecedented opportunities for a new generation of neutron studies[30].

More widely at the Harwell Science and Innovation Campus, an engineering centre is planned at the new Research Complex at Harwell. By bringing together large scale facilities like the ISIS neutron source, Diamond light source and the Central Laser Facility into a collaborative framework, the user community will be able to undertake new scientific and applied research. mt

REFERENCES

1. Zhang, S. Y., and Korsunsky, A. M., Proceedings of CM 2008/MFPT 2008, Edinburgh, (2008).
2. Sirohi, J., and Chopra, I., *J. Intelligent Matl Systems Structs.* (2000) **11** 246
3. Sciammarella, C. A., *Experimental Mechanics* (1982) **22** 418
4. Chu, T. C., *et al., Experimental Mechanics* (1985) **25** 232
5. Xu, P. G., *et al., Materials Science and Engineering A* (2006) **435** 46
6. Tomota, Y., *et al., Nuclear Instruments and Methods in Physics Research A*, (2009) **600** 313
7. Xu, P. G., *et al., Materials Transactions* (2008) **49**, 2033.
8. Tomota, Y., *et al., Acta Materialia* (2004) **52** 5737
9. Xu, P. G., *et al., ISIJ International* (2008) **48** 1609
10. Xu, P. G. *et al., ISIJ International* (2008) **48** 1618
11. James, J. A., *et al., Physica B, Condensed Matter* (2004) **350** 743
12. Hutchings, M. T., et al., Introduction to the Characterization of Residual Stress by Neutron Diffraction. Boca Raton: CRC Press, Taylor and Francis (2005).
13. Fitzpatrick, M. E., and Lodini, A., Analysis of Residual Stress by Diffraction using Neutron and Synchrotron Radiation. London: Taylor and Francis. (2003).
14. Santisteban, J. R., *et al.,* J. Appl. Cryst. (2006) **39** 812
15. Hodgson, P. D., *et al., Materials Science Forum* (1998) **63** 284
16. Dong, H., and Sun, X. J., *Current Opinion in Solid State and Materials Science* (2006) **9** 269
17. Xu, P.G., *et al., CAMP-ISIJ* (2009) **22** 539
18. Oliver, E. C., *et al., Acta Mater.* (2003) **51** 6453
19. Oliver, C., *et al., Meas. Sci. Technol.* (2008) **19** 034019
20. Marsh, G., *Reinforced plastics* (2005)
21. Liljedahl, C. D. M., *et al.,* (2009) In preparation
22. Turner, P. A., *et al., Int. J. Plasticity* (1995) **11(3)** 251
23. Turski, M., *et al., Zeit. Kristallographie* (2008) **27** 231
24. Korsunsky, A. M., *et al., J. Strain Anal.* (2009) **44** 159
25. Kockelmann, W., *et al., Nuclear Inst. Meth. Physics Research A* (2007) **578** 421
26. Zhang, S. Y., *et al., Applied Physics A* (2009), Submitted
27. Abbey, B., *et al., Procedia Engineering, Mesomechanics 2009* conference, Oxford (2009)
28. Vorster, W. J. J., *et al., J. Strain Anal.* (2009) **44** 71
29. Siano, S., *et al., Archaeometry* (2006) **48** 77
30. Kockelmann, W., *et al., IMAT outline specifications, STFC* (2009)